JOURNAL OF APPLIED ELECTROCHEMISTRY 19 (1989) 495–499

Voltage delay during constant-current or constant-resistance discharge of Mg–MnO_2 dry cells: a comparative study

S. R. NARAYANAN, S. SATHYANARAYANA*

Department of Inorganic and Physical Chemistry, Indian Institute of Science, Bangalore 560 012, India

Received 20 September 1988; revised 5 December 1988

A theoretical approach has been developed to relate the voltage delay transients of the Mg–MnO_2 dry cell observed during discharge by two commonly employed modes, viz., (1) at constant current, and (2) across a constant resistance. The approach has been verified by comparison of experimentally obtained transients with those generated from theory. The method may be used to predict the delay parameters of the Mg–MnO_2 dry cell under the two modes of discharge and can, in principle, be extended to lithium batteries.

1. Introduction

The magnesium–manganese dioxide dry cell (Mg–MnO_2) is a representative of the class of primary batteries with high energy density and long shelf life. The long shelf life of the Mg–MnO_2 dry cell is due to the presence of a passive film which protects the highly reactive Mg from spontaneous corrosion. This protective passive film, however, breaks down on initiating cell discharge, allowing free anodic dissolution of magnesium.

During the initial moments of discharge of the Mg–MnO_2 dry cell, the cell voltage follows a typical course shown schematically in Fig. 1. That is, at the instant t_a of initiation of discharge, the voltage falls appreciably from the open-circuit value V_i, and then gradually rises to attain a steady state closed-circuit value V_∞. The delayed attainment of a steady state cell voltage following initiation of discharge is termed 'voltage delay' or 'delayed action', and the time elapsed before a particular value of cell voltage is reached is termed the 'delay time'. The delayed action behaviour is characteristic of the Mg–MnO_2 dry cell and such other cells where the anode is covered by an insulating passive film (e.g. Li and Al batteries). The magnitude of the delay time is crucial to the practical application of these cells and it is desirable that the delay time is kept to the minimum possible.

The main features of the voltage delay transient of the Mg–MnO_2 dry cell are fairly well understood [1–3]. The delay time measured for a chosen closed-circuit cell voltage is dependent on the discharge current density, temperature of the cell during discharge and the properties of the film-covered Mg/electrolyte interface [4–6]. In particular, the voltage delay characteristics are significantly dependent on the mode of discharge. The discharge of the Mg–MnO_2 dry cell is usually carried out by two modes, schematically represented in Fig. 2. These are: (i) discharge at constant current, J (CC discharge); (ii) discharge across a constant resistance, R_L (CR discharge).

CC discharge is widely used as it permits easy evaluation of the capacity and internal resistance of the cells. CR discharge represents the practical application of the cells, and the discharge current varies throughout the course of discharge. The delay time (measured at any particular voltage) by CR discharge is four to five times that observed by CC discharge even when the discharge current observed in the steady state by CR discharge is equal to the constant discharge current by CC discharge (Figs 3 and 4). Although these differences may be attributed to the varying discharge current during CR discharge as against a constant-discharge current in CC discharge, it would be useful to obtain a relationship between the voltage delay characteristics observed by these two widely used modes. In particular, it would be desirable to be able to predict the delay time for any chosen value of R_L or J, given the voltage delay transient under any other condition of R_L or J.

In the present study, a theoretical approach has been developed to obtain the voltage delay characteristic for CC discharge from a delay transient experimentally obtained by CR discharge. The approach has been verified by comparison of the theoretically constructed voltage delay transients with those obtained by experiment.

2. Theoretical analysis

2.1. *Physical model for delayed action*

On initiation of discharge, the insulating passive film on Mg resists the flow of discharge current leading to

* Author to whom correspondence should be addressed.

0021-891X/89 $03.00 + .12 © 1989 Chapman and Hall Ltd.

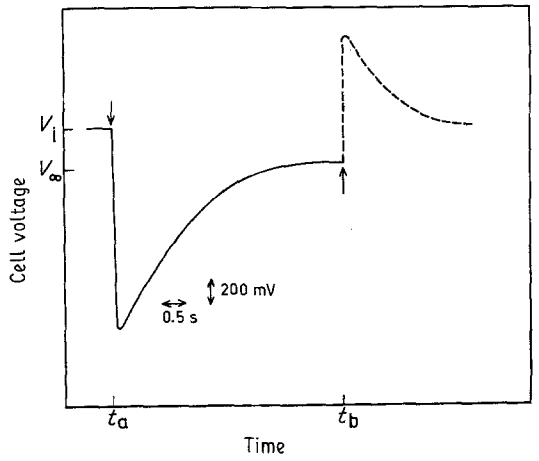

Fig. 1. Schematic of the dependence of cell voltage on time during the initial moments of discharge, and subsequent open-circuit recovery, of CD-size Mg–MnO_2 dry cell. Discharge rate: 10^{-3} A; t_a: time of initiation of discharge; t_b: time of termination of discharge; V_i: open-circuit cell voltage; V_∞: steady state closed-circuit cell voltage. Dashed lines indicate open-circuit conditions. Arrows indicate moment of initiation and termination of discharge.

an instantaneous cell voltage drop. The resulting high-electric field across the film-covered Mg/electrolyte interface, causes dielectric breakdown of the passive film leading to anodic dissolution of magnesium at weak spots in the film. The anodic product thus formed creates dilatation stresses causing rupture of the film, and permitting unhindered anodic dissolution of magnesium. The cell voltage then rises to a value V_∞, characteristic of the steady state polarization of the magnesium anode at that discharge current (Fig. 1). Subsequently, on interruption of discharge, the open-circuit cell voltage shoots to a value characteristic of the high negative potential of the film-free Mg anode. Then, with the onset of passivation, the cell voltage recedes to the value, V_i, that prevailed prior to the initiation of discharge [1–3]. This physical model leads to the following analysis of the voltage delay transients.

2.2. *Contribution of anode film resistance to the internal resistance of the Mg–MnO_2 dry cell*

The voltage delay transient (Fig. 3) represents the effect of a varying internal resistance of the cell during the initial moments of discharge at constant current. In general, the internal resistance of the Mg–MnO_2 dry cell R_i, has contributions from: (i) ohmic resistance of the cathode, electrolyte, separator and anode film; (ii) polarization effects at the anode and cathode. The MnO_2 electrode, being a large-area porous electrode, may be considered non-polarizable and consequently polarization effects at the cathode may be neglected. Under these conditions, R_i is given by

$$R_i = R_f + R_{ct,a} + R_{mt,a} + R_\Omega \qquad (1)$$

where R_f is the anode film resistance, $R_{ct,a}$ the charge transfer resistance for anodic dissolution of magnesium, $R_{mt,a}$ the mass transfer resistance at the anode and R_Ω the sum of the ohmic resistance of the cathode, electrolyte and separator.

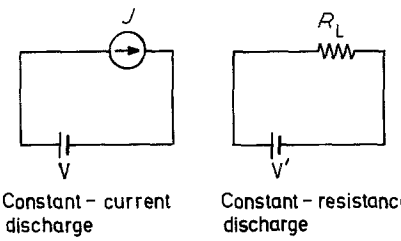

Fig. 2. Schematic description of the two commonly employed modes of discharge, viz. constant-current discharge at constant current, J, and constant-resistance discharge across a constant resistance, R_L. V and V' represent the closed-circuit cell voltage during discharge.

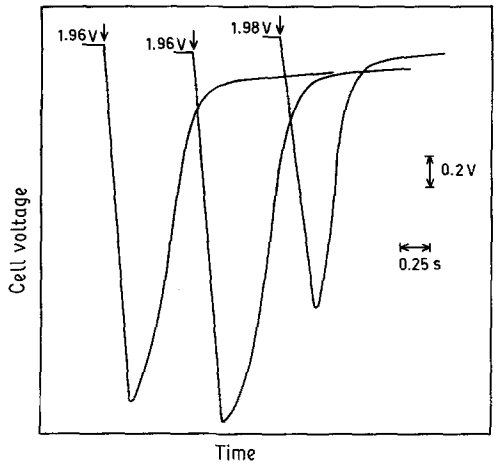

Fig. 3. Cell voltage transients observed during discharge of three Mg–MnO_2 dry cells at a constant current of 0.1 A at 0° C. Arrows indicate the moment of initiation of discharge. The open-circuit voltage is shown for each cell preceding the arrow.

In the absence of anode film breakdown it has been shown [4] that the internal resistance of the Mg–MnO_2 dry cell is governed entirely by the anode film resistance, R_f. The typical values of R_f under these conditions is $10^7\ \Omega$ for a CD-size cell. With progressive damage to the passive film caused by discharge current densities in the range 10^{-6}–10^{-3} A cm^{-2} (anode current density), R_i falls and reaches ultimately a value of 0.5–1.0 Ω (Fig. 5). It has been shown [1, 6] that $R_{ct,a}$ is typically 0.1 Ω and $R_{mt,a}$ is negligible during the initial moments of discharge, as sufficient supply of electrolyte is available. However R_Ω from a.c. impedance measurements [5] is in the range 0.5–1.0 Ω. Consequently, neglecting $R_{ct,a}$ and $R_{mt,a}$, R_i may be given by

$$R_i = R_f + R_\Omega \qquad (2)$$

Since R_Ω is a small and relatively constant value of 0.5–1.0 Ω, the large variation in R_i during the course of the voltage delay transients (Figs 3 and 4) is entirely determined by R_f, which decreases as breakdown of the passive film occurs. Ultimately, when the film break-down is complete, R_f becomes negligible and R_Ω governs the value of R_i.

2.3. *Assumptions and relationships*

Based on the physical model (Section 2.1) for anode film breakdown, and the contribution of the anode

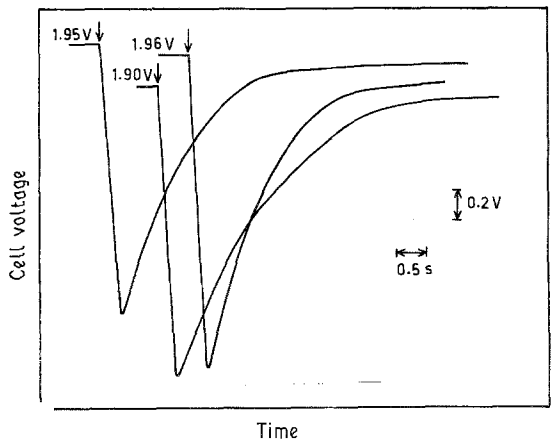

Fig. 4. Cell voltage transients observed during discharge of three Mg–MnO_2 dry cells across a constant resistance of 18 Ω at 0° C. Arrows indicate the moment of initiation of discharge. Open-circuit voltage is shown for each cell, preceding the arrow.

film resistance to the internal resistance of the cell (Section 2.2), the following assumptions may be made: (i) As damage to the anode film arises from dilatation stresses caused by accumulation of anodic product, the extent of such film damage should be proportional to the quantity of electricity delivered by the cell during the specified discharge interval. (ii) A particular quantity of electricity – and therefore the anodic product – would cause the same extent of film damage, and consequently, result in the same decrease in internal resistance of the cell, independent of the rate of discharge (within limits of practically significant discharge rates). (iii) The non-faradaic contribution to the discharge current during the course of the voltage delay transient may be estimated from the value of $C(dV/dt)$, where C is the effective capacitance observed between the terminals, and V the closed-circuit cell voltage. For a CD-size Mg–MnO_2 dry cell, $C \approx 10\,\mu F\,cm^{-2}$ [5], anode area 100 cm^2 and $dV/dt \approx 0.5\,V\,s^{-1}$ (Figs 3 and 4). The value of non-faradaic current is thus $\sim 5 \times 10^{-4}$ A. This is less than 1% of the values of discharge current employed in the practical application of the cells (viz. 0.05–0.5 A). Thus the non-faradaic contribution may be ignored in this analysis.

With these assumptions, the relationship between the voltage delay transients observed during discharge at constant current and across a constant resistance may be deduced as follows.

Let V_i be the open-circuit cell voltage prior to the initiation of discharge. Let V and V' be the closed-circuit cell voltages during CC discharge and CR discharge, respectively. Let J be the constant discharge current during CC discharge. Let R_L be the constant resistance across which CR discharge occurs. The instantaneous discharge current J' for CR discharge is then given by

$$J' = \left(\frac{V'}{R_L}\right) \tag{3}$$

Now, an instantaneous internal resistance parameter R may be defined for CC discharge as

$$R = \frac{V_i - V}{J} \tag{4}$$

The basis for such a definition is as follows. In the absence of anode film breakdown it has been shown [1] that when $V = V_\infty$, $R = R_i$. Similarly, when film breakdown is complete, i.e. $V = V_\infty$ (Fig. 1), again R calculated by Equation 4 is very close to the value of R_i obtained by d.c. methods. For example, from Fig. 3, the value of R in the steady state is approximately 0.3 Ω. Consequently, R may be used as an operational internal resistance parameter in the analysis of the voltage delay transients. Similarly, a parameter R' may be defined for CR discharge as

$$R' = \left(\frac{V_i - V'}{V'}\right) R_L \tag{5}$$

The charge Q, withdrawn after a time t, during CC discharge is given by

$$Q = Jt \tag{6}$$

Similarly, after a time t', the charge withdrawn by CR discharge Q' is given by

$$Q' = \int_0^{t'} \left(\frac{V'}{R_L}\right) dt' \tag{7}$$

By assumption (ii), when $Q = Q'$, the same value of internal resistance of the cell is attained in both the two modes of discharge. Equating therefore R and R', we have from Equations 4 and 5

$$V = V_i - JR_L\left(\frac{V_i - V'}{V'}\right) \tag{8}$$

and from Equations 6 and 7

$$t = \frac{1}{J}\int_0^{t'} \left(\frac{V'}{R_L}\right) dt' = \frac{Q'}{J} \tag{9}$$

Equations 8 and 9 relate the voltage and time coordinates (V, t) and (V', t') on the delay transients observed in CC discharge and CR discharge, respec-

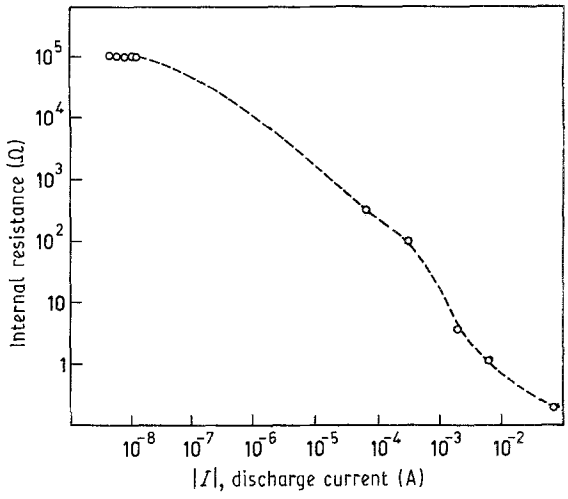

Fig. 5. Typical variation of internal resistance with discharge current at 23° C of Mg–MnO_2 dry cell (CD-size; anode area 100 cm^2) in the constant-current discharge mode.

tively. For a particular coordinate (V', t') on the delay transient experimentally obtained by CR discharge, Q' may be evaluated (Equation 7) by graphical integration. Then, for a chosen value of J, a point t on the delay transient for CC discharge may now be calculated by Equation 9. Also, from Equation 8, the point V corresponding to V' may be evaluated. This way the entire delay transient for CC discharge may be generated from the delay transient obtained for CR discharge.

The calculation may be repeated for the desired values of J. Similarly, when the delay transient experimentally obtained by CC discharge is available, that for CR discharge may be calculated by the following method. For a chosen coordinate (V, t), V' may be calculated for a desired value of R_L from Equation 8. To calculate t' it is necessary to approximate V' as a function of t'. If a linear relationship between V' and t' is assumed at this stage, Equation 7 becomes

$$Q' = \frac{V't'}{2R_L}$$

and Equation 9 may be written as

$$t' = \frac{2R_L Jt}{V'} \qquad (10)$$

t' may now be evaluated. This way the entire voltage transient for CR discharge may be theoretically generated.

3. Experimental verification

The CD-size Mg–MnO_2 dry cells employed in this work were manufactured by M/s Bharat Electronics Ltd, India. Voltage delay transients were recorded for $R_L = 18\,\Omega$ (Fig. 4) and $J = 0.1$ A (Fig. 3), for 3 cells in each case. The temperature of the cell during discharge was maintained at $0 \pm 0.5°$ C employing a water–polyethylene glycol mixture in a bath cryostat. The electrical circuit employed is shown in Fig. 6. An electrometric amplifier (input impedance $10^{12}\,\Omega$) was used for the voltage measurements so that the sensing currents are small enough as not to damage the protective passive film prior to the initiation of discharge [4].

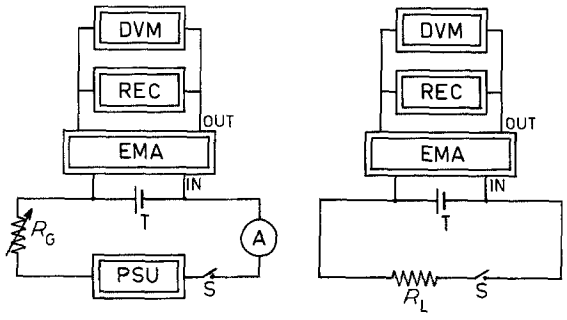

Fig. 6. (a) Electrical circuit for the discharge of Mg–MnO_2 dry cell at constant current (accompanied by anode film breakdown) and observation of cell voltage transients. (b) Electrical circuit for discharge of Mg–MnO_2 dry cell across constant resistance, R_L (accompanied by anode film breakdown) and observation of cell voltage transient. T: test cell; EMA: electrometric amplifier (Wenking PPT 75; input impedance greater than 10^{13}); REC: recorder (Rikadenki WE 201); DVM: digital voltmeter (HIL-230); PSU: power supply unit (Aplab LVA 30/3); R_G: current limiting resistance (Rheostat 100, 2A); A: ammeter (Motwane 8X MK III); R_L: constant load resistance (Toshniwal Decade resistance box); S: switch.

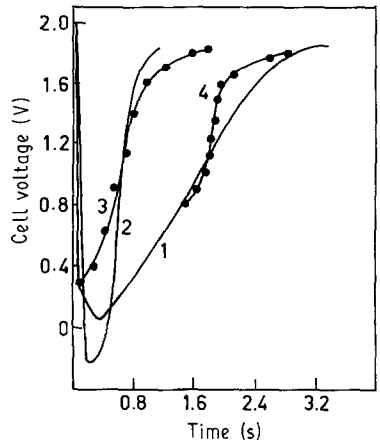

Fig. 7. Comparison of experimental and theoretical cell voltage transients for Mg–MnO_2 dry cell (CD-size) at 0° C under discharge conditions causing anode film breakdown. (1) Constant-resistance discharge ($R_L = 18\,\Omega$) – experimental; (2) constant-current discharge ($I = 0.1$ A) – experimental; (3) constant-current discharge ($I = 0.1$ A) – theoretically derived from curve 1; (4) constant-resistance discharge ($R_L = 18$ ohm) – theoretically derived from curve 2.

The voltage delay transients for $J = 0.1$ A and for $R_L = 18\,\Omega$ have been theoretically generated by the procedure described in Section 2.3 and are compared with the corresponding experimental transients in Fig. 7. The theoretical curves follow the course of the experimental transients in the rising region of the transients (which corresponds to film breakdown). In particular there is significant agreement between theory and experiment in the magnitudes of delay time in the voltage range of practical importance, viz. 0.8–1.6 V.

The agreement between theory and experiment may be possibly improved by correcting the discharge current for the non-faradaic contribution, and inclusion of heat-induced effects at the Mg/solution interface, caused by the passage of current (this being different for CC discharge and CR discharge).

4. Conclusion

The approach developed to relate the voltage delay transients during 'constant-current discharge' and 'constant-resistance discharge' of the Mg–MnO_2 dry cell makes possible interconversion of data obtained by these two modes. This would be of practical value in predicting the delay characteristics during discharge by one of the modes, given experimental data obtained by the other mode. The method can be extended, in principle, to lithium batteries.

References

[1] B. V. Ratnakumar and S. Sathyanarayana, *J. Power Sources* **10** (1983) 219.

[2] S. Sathyanarayana and B. V. Ratnakumar, *J. Power Sources* **10** (1983) 243.

[3] B. V. Ratnakumar and S. Sathyanarayana, *J. Power Sources* **12** (1984) 39.
[4] S. R. Narayanan and S. Sathyanarayana, *J. Power Sources* **15** (1985) 27.
[5] S. R. Narayanan and S. Sathyanarayana, *J. Power Sources* **24** (1988) 51.
[6] S. R. Narayanan and S. Sathyanarayana, *J. Power Sources* **24** (1988) 295.